

# The Mechanical Properties of Polyvinyl Butyral (PVB) at High Strain Rates

Xihong Zhang<sup>1\*</sup>, Hong Hao<sup>2</sup>, Yanchao Shi<sup>3</sup>, Jian Cui<sup>3</sup>

1. School of Civil, Environmental and Mining Engineering, the University of Western Australia, 35 Stirling Highway, Crawley WA 6009, Australia
2. Tianjin University and Curtin University Joint Research Center of Structural Monitoring and Protection, School of Civil and Mechanical Engineering, Curtin University, Kent St., Bentley WA 6102, Australia
3. Tianjin University and Curtin University Joint Research Center of Structural Monitoring and Protection, Tianjin University, China

\*email: xihong.zhang@uwa.edu.au

Phone: +61 8 6488 7199

## Abstract

Polyvinyl Butyral (PVB) has been largely used as an interlayer material for laminated glass to mitigate the hazard from shattered glass fragments, due to its excellent ductility and adhesive property with glass pane. With increasing threats from terrorist bombing and debris impact, the application of PVB laminated safety glass has been extended from quasi-static loading to impact and blast loading regimes, which has led to the requirement for a better understanding of PVB material properties at high strain rates. In this study, the mechanical properties of PVB are investigated experimentally over a wide range of strain rates. Firstly, quasi-static tensile tests is performed using conventional hydraulic machine at strain rates of  $0.008\sim 0.317s^{-1}$ . Then high-speed tensile test is carried out using a high-speed servo-hydraulic testing machine at strain rates from  $8.7s^{-1}$  to  $1360s^{-1}$ . It is found that under quasi-static tensile loading, PVB behaves as a hyperelastic material and material property is influenced by loading rate. Under dynamic loading the response of PVB is characterized by a time-dependent nonlinear elastic behavior. The ductility of PVB reduces as strain rate increases. The testing results are consistent with available testing data on PVB material at various strain rates. Analysis is made on the testing data to form strain-rate dependent stress-strain curves of PVB under tension.

**Keywords:** PVB; dynamic material property; high-speed tensile tests.

## 1 1. Introduction

2 PVB, short for Polyvinyl Butyral, is a polymer material with outstanding mechanical  
3 properties and excellent optical clarity, which has been primarily used as an interlayer  
4 material for laminated glass in the field of construction and automobiles. In the manufacture  
5 of laminated glass, normally two glass panes are bonded by a transparent polymer interlayer.  
6 Due to the low shear stiffness, before glass crack the composite pane carries lateral loads  
7 mainly through the two glass plies (Figure 1a). After glass breaks, the interlayer comes into  
8 effect. It holds the shattered glass splinters together and prevents them from flying into the  
9 occupied area. Post-glass breakage, the glass ply only bears the compressive force, while the  
10 PVB interlayer bridging between the shattered glass fragments carries the tensile force  
11 (Figure 1b). Although analysis and design of laminated glass against conventional quasi-static  
12 and low-rate dynamic loading such as wind is well developed, the behavior of a laminated  
13 pane under high-rate dynamic loading such as blast and impact is relatively less understood.  
14 Despite many researches onto the response of laminated pane under such loadings being  
15 reported recently [1-4], the mechanical behavior of PVB interlayer at high-strain rates still  
16 needs be investigated for better predictions of the laminated glass window responses  
17 subjected to blast and impact loads.

18 The mechanical behavior of PVB has been proven to be complicated. It is highly nonlinear,  
19 time-dependent, and being capable of undergoing substantial extension. The compressive  
20 behavior of PVB under quasi-static and dynamic loadings was exclusively studied [5, 6]. The  
21 stress-strain curves at strain rates from  $4 \times 10^{-4} \text{s}^{-1}$  to  $4 \times 10^{-2} \text{s}^{-1}$  for quasi-static state and at  
22 strain rates from  $700 \text{s}^{-1}$  to  $4500 \text{s}^{-1}$  were obtained using conventional testing machine and  
23 Split Hopkinson Pressure Bar (SHPB) technique, respectively. Time-dependent viscoelastic  
24 characteristics were observed for PVB under impact. A two-stage behavior, i.e. 'compaction  
25 stage' and 'hardening stage', was introduced to describe the response of PVB under dynamic  
26 compression. Through comparison with Ogden model, it was found that Mooney-Rivlin  
27 model well describes PVB compressive behavior [5].

28 The behavior of PVB under tension is more to the interest of studying PVB laminated  
29 glass windows, as PVB interlayer is quite thin and only takes tensile force in the composite.  
30 The small-strain behavior of PVB has been investigated intensively to analyze the pre-glass  
31 crack response of laminated pane under quasi-static loading such as wind pressure. A  
32 viscoelastic model is generally introduced for PVB material with a generalized Maxwell series  
33 to account for the time-dependent shear modulus [7, 8]. Dynamic mechanical analysis found

1 that PVB has a rubbery modulus of the order of 1MPa and a glassy tensile modulus in the  
2 order of 1GPa [9]. The influence of temperature variation is considered by using the  
3 Williams-Landel-Ferry equation to shift the shear modulus of different temperatures.  
4 Transition between a rubbery material to a glass-like material occurs at a temperature of 5°C  
5 to 40°C [9].

6 The mechanical behavior of PVB at large strain has been studied through laboratory  
7 testing at both the quasi-static and dynamic states. For the quasi-static region, Iwasaki et al.  
8 [10] tested 0.76mm thick PVB specimen and derived stress-strain curves at strain rates from  
9  $0.0067s^{-1}$  to  $0.2s^{-1}$ . Bennison et al. [11] obtained stress-strain curves of PVB at strain rate  
10  $0.07s^{-1}$  and  $0.7s^{-1}$ . Liu et al. [6] investigated PVB tensile properties at strain rates of  $0.004s^{-1}$ ,  
11  $0.02s^{-1}$ ,  $0.04s^{-1}$ , and  $0.08s^{-1}$ . The above tests all found that PVB shows viscoelastic material  
12 property under low-speed tension, and the response is influenced by loading speed.  
13 Dynamic tensile tests found the dynamic profile of PVB differs significantly from its quasi-  
14 static behavior. Iwasaki et al. [10] presented the stress-strain curve of PVB at a strain rate of  
15  $118s^{-1}$ . It depicts that under dynamic loading PVB exhibits elasto-plastic material property  
16 with a steep initial rise in stress followed by a decrease in stress increment. A few dynamic  
17 tensile tests have been reported lately on PVB material at various strain rates. For instance,  
18 using a servo-hydraulic testing machine Bennison et al. [11] tested PVB tensile strength at  
19 strain rates of  $8s^{-1}$  and  $89s^{-1}$ . With an Imateck impact test machine, Morison [12] carried out  
20 drop weight tests and obtained PVB tensile profile at strain rates from  $33.5s^{-1}$  to  $278s^{-1}$ .  
21 Hooper et al. [9] also reported their testing data on PVB at strain rates from  $2s^{-1}$  up to  $400s^{-1}$ .  
22 The dynamic testing results found PVB tensile response is characterized with time-  
23 dependence. The initial modulus, yield stress, and failure stress will be amplified at  
24 increased strain rates. However, as strain rate increases PVB becomes less ductile with  
25 diminishing failure strain. The influence of temperature has also been investigated. Morison  
26 extended his drop weight tests on PVB at room temperature to another two temperatures,  
27 i.e. 5°C and 35°C. It was found that at room temperature despite PVB exhibits elasto-plastic  
28 behavior which is analogous to yield in metal, the response remains viscoelastic as the  
29 additional deformation in the specimen is gradually recoverable once unloaded. At lower  
30 temperature, PVB still behaves elasto-plastically but associated with smaller hardening  
31 stiffness. At elevated temperature, the stress-strain curve is much closer to linear  
32 viscoelastic.

1 With more and more applications of PVB laminated glass into retrofits against shock and  
2 impact loading where the strain rate that material experiences is high, a thorough  
3 investigation of PVB mechanical properties at a wider strain rate range, especially at high-  
4 strain rates beyond the current available testing data is needed. In this study, we carry out  
5 uniaxial tensile tests on PVB material at a wide range of strain rates. Firstly, low-speed  
6 tensile test is performed on 0.76mm thick PVB specimen to investigate its quasi-static  
7 behavior at strain rates of  $0.008s^{-1}$  to  $0.317s^{-1}$ . Then, high-speed tensile test is carried out  
8 using a high-speed servo-hydraulic testing machine to study PVB dynamic response at strain  
9 rates from  $8.6s^{-1}$  to  $1360s^{-1}$ . The testing data are analyzed. They are used together with  
10 previous testing results obtained by other researchers on PVB to derive a strain-rate-  
11 dependent stress-strain relationship for PVB.

## 12 **2. Theory and Methodology**

### 13 2.1 Testing systems

14 Experimental techniques commonly used to determine material tensile properties at  
15 different strain rates include conventional screw driven load frame, servo-hydraulic machine,  
16 pendulum or drop weight impact system, high-speed servo-hydraulic machine, and Split-  
17 Hopkinson Pressure Bar system. The conventional testing systems including the screw driven  
18 load frame and conventional servo-hydraulic machine can normally test material tensile  
19 strength at a strain rate up to  $1s^{-1}$ . Split-Hopkinson Pressure Bar (SHPB) is commonly used to  
20 determine material strength at high strain rates ( $\dot{\epsilon} \geq 100s^{-1}$ ). In determining the material  
21 tensile properties, the tensile SHPB usually requires the testing specimen to be firmly glued  
22 on both ends respectively to the incident and transmitter bars to ensure the tensile stress  
23 wave can travel through the specimen before it fractures. It is therefore not ideal to test  
24 polymer materials like PVB, as the glue could significantly alter material properties. The  
25 pendulum or drop weight impact system and the high-speed servo-hydraulic machine have  
26 been widely used to determine material strength at strain rate above  $1s^{-1}$ . Dog-bond shaped  
27 specimens similar to those used for quasi-static tests are most commonly adopted for the  
28 dynamic tensile tests. Due to inherent difficulties, the strain rates that can be achieved by a  
29 drop weight impact machine is usually limited to below  $100s^{-1}$ . Moreover, during a test the  
30 velocity of the actuator is interacted with the response of the specimen. It is difficult for the  
31 drop weigh impacter to maintain a constant velocity. In this study, servo-hydraulic and high-  
32 speed servo-hydraulic machines are used to perform the low-speed and high-speed tensile

1 tests. The testing setups and machine information are described in details in section three  
2 and four.

### 3 2.2 Testing requirements for high-speed tests

4 To ensure the validity of testing data for a material test, it is critical to assure the  
5 specimen is under the state of stress equilibrium. For low-speed tests, the specimens are in  
6 quasi-static equilibrium as comparing with the loading duration there is more than sufficient  
7 time for elastic wave to travel back and forth many times inside the specimen. For high-  
8 speed tests, to achieve the state of stress equilibrium is much more difficult since the  
9 loading time can be much shorter. In a dynamic test, a state of dynamic equilibrium is  
10 usually pursued, where a minimum number of elastic waves are required to propagate  
11 through the specimen. To estimate the time for one stress wave to travel a round trip in the  
12 specimen the following relation can be utilized

$$t = \frac{2L}{c} \quad (1)$$

13 where L is the specimen length between the clamping grips; and c is the elastic stress wave  
14 velocity in the testing material. The one-dimensional longitudinal wave velocity in an  
15 isotropic material can be estimated by the relation

$$c = \sqrt{\frac{E}{\rho}} \quad (2)$$

16 where  $\rho$  is the density of the material, and E is the Young's modulus.

17 To reach dynamic stress equilibrium, a SHPB test normally requires at least three  
18 reverberations of the loading wave in the specimen [13, 14]. Based on dynamic tensile tests  
19 using a high-speed servo-hydraulic machine on different plastic materials, it has been found  
20 the criterion for a valid SHPB test is also applicable to dynamic direct tensile test [15]. The  
21 daft standard of the Society of Automotive Engineers on high strain-rate tensile test for  
22 automotive plastics requires at least 10 elastic reflected waves propagating through the  
23 specimen from the time of loading to the time of yield. There is no quantitative criterion in  
24 the open literature yet defining the exact number of reflected stress wave in the specimen  
25 to achieve dynamic equilibrium for a uniaxial tensile test.

26

### 1 **3. Low-Speed Tests**

#### 2 3.1 Test setup

3 PVB specimens for the low-speed tests were made from 0.76mm thick PVB sheets using  
4 the punch as shown in Figure 2. The specimen is in a dog-bone shape with a central testing  
5 gauge of 40mm in length. Plastic tabs are attached to the tails of the specimen to ensure the  
6 thin PVB film will not slip from the clamping jaw. It is worth noting that due to the very low  
7 thickness of the specimen, in the preliminary testing even with the added plastic tabs the  
8 specimen would still slip. Worse still, any fixing glue applied directly onto the PVB specimen  
9 would alter the material property and make it brittle. After some trials, an additional layer of  
10 soft cloth (as shown in Figure 2) is introduced between the plastic tab and specimen.  
11 Satisfactory clamping was achieved in this manner and good testing results were obtained.

12 The low-speed test was performed in two stages. In the first stage, uniaxial tensile test  
13 was carried out on a Baldwin universal testing system with additional clamping device to fix  
14 the specimens, and an external load cell to measure the applied force (Figure 3a). The  
15 Baldwin machine is a servo-hydraulic system where the actuator velocity is controlled  
16 manually with applied oil pressure. 8 PVB specimens were tested on this machine with  
17 measured strain rates varying from  $0.008s^{-1}$  to  $0.043s^{-1}$ . In the second stage, an Instron  
18 hydraulic testing machine UTS-5982 as shown in Figure 3b is utilized. The actuator of the  
19 machine can maintain a computer controlled constant pulling speed of 50mm/min to  
20 1016mm/min with a maximum stroke length of 1430mm. The applied force and the  
21 deformation of the PVB specimen were monitored using an inbuilt load cell and  
22 extensometer on top of the upper clamp. Another 15 specimens were tested on the Instron  
23 machine at four crosshead velocities, i.e. 50mm/min, 250mm/min, 500mm/min, and  
24 800mm/min, corresponding to nominal strain rates of  $0.0198s^{-1}$ ,  $0.0992s^{-1}$ ,  $0.1984s^{-1}$ , and  
25  $0.3175s^{-1}$ . The room temperature during the test was around  $23^{\circ}C \pm 5^{\circ}C$ .

#### 26 3.2 Results

27 The machine crosshead displacement is used to evaluate the elongation of the specimen.  
28 Specimen strain is determined by using the elongation dividing its original length. The strain  
29 rate that specimen experienced is derived by differentiating strain time history. Figure 4  
30 shows a sample strain-rate time history derived from the machine crosshead displacement  
31 (specimen G04). As can be observed, the machine quickly reaches the designed testing  
32 velocity and the specimen is pulled at a constant velocity until the specimen fractured as  
33 indicated. Engineering stress-strain curves obtained from the low-speed tensile tests are

1 shown in Figure 5. As shown, under low-speed tension PVB displays viscoelastic property.  
2 The stress increases with strain in an exponential form. The stress increases gradually with  
3 the strain in the beginning, and then grows steeper as strain increases. The behavior of PVB  
4 under low-speed tensile loading shows strain-rate dependence. As show in Figure 5, the  
5 inclination of the stress-strain curves becomes steep as the tensile speed increases. The  
6 failure strains of PVB at low-speed test are generally over 200%. But as pulling speed  
7 increases, PVB becomes brittle and the failure strains become smaller. For instance, when  
8 the strain rate was  $0.02s^{-1}$ , the specimen failed with an ultimate strain of 245%. As strain  
9 rate increased to  $0.317s^{-1}$ , the failure strain dropped to 175%. The testing results on PVB  
10 specimen under low-speed tension are summarized in Table 1. It should be noted that  
11 because of the non-uniform elongation of material around the shoulders of the specimen,  
12 the strain derived using machine crosshead displacement could introduce some deviation.  
13 But since the length of the shoulder is relatively short comparing with the entire length of  
14 the specimen, the deviation is believed to be small.

#### 15 **4. High-Speed Dynamic Tests**

16 The high-speed tensile test was carried out at the Tianjin University and Curtin University  
17 Joint Research Center. The room temperature during the test was about  $30^{\circ}C \pm 3^{\circ}C$ . A high-  
18 speed servo-hydraulic test machine was utilized with an actuator pulling speeds ranging  
19 from 0.1m/s to 20m/s. The tests discovered the dynamic material properties of PVB at strain  
20 rates ranging from approximately  $8.6s^{-1}$  to  $1360s^{-1}$ .

##### 21 **4.1 Test setup**

22 An Intron VHS testing system (VHS 160-20) is utilized to carry out the high-speed test. The  
23 machine is comprised of a fast jaw grip which accelerates upwards in the direction of tension  
24 (Figure 6a). As soon as the jaw reaches the designed testing velocity, a wedge will be  
25 knocked out to release the sprung grip to grab the upper clamping bar and pull it up at the  
26 designed testing velocity till failure. The actuator of the machine can maintain a constant  
27 velocity from 1mm/s to 1m/s under closed loop control, and a maximum velocity of 25m/s  
28 under open loop control. Specially designed lightweight clamps as shown in Figure 6b are  
29 designed and made to fix the specimens. The upper clamp comprises of a 350mm long arm  
30 which is riveted to a 60mm by 60mm alloy tab. The fast jaw travels freely along this arm and  
31 grab it when it reaches the designed testing velocity. 4 plastic bolts are used to fasten  
32 another alloy tab to clamp the tail of the PVB specimen firmly. The lower clamp has the  
33 same structure but with a shorter alloy arm to be fixed into the bottom grip head. The

1 clamps are made of magnesium alloy (AZ31B). The density of the alloy is  $1770\text{kg/m}^3$ . To  
2 minimize the influence of inertia effect, the clamps are only 1mm thick. The yield strength of  
3 alloy is about 200MPa under uniaxial tension, and the Young's modulus is 44.8GPa. The high  
4 strength and large modulus compared to those of PVB assure the clamping bars will not  
5 yield nor result in large elongation during the test.

6 The PVB specimens for the high-speed tensile tests were sampled from 0.76mm PVB  
7 sheet used for laminated glass. Due to the low strength of the material, eight layers of  
8 0.76mm PVB sheets were stacked together, heated to about  $70^\circ\text{C}$  and then pressed by a  
9 roller to squeeze out the air or any blister. The process follows the manufacture procedure  
10 of producing laminated glass panes. In such a manner,  $6.08\text{mm}\pm 0.05\text{mm}$  thick PVB sheets  
11 were made. Using a die cut, the 6.08mm thick PVB sheets were machined into the geometry  
12 as shown in Figure 7. The 10mm central testing gauge was marked with thin black lines with  
13 a permanent marker to enable optical strain measurement with high-speed camera. The  
14 dog-bone shape specimen has two long tails to be clamped by the alloy tabs. To avoid  
15 slippage of specimen being pulled out of the clamping tabs, two additional plastic tabs were  
16 added to the tails of the PVB specimens.

17 A linear variable differential transducer (LVDT) embedded in the fast jaw was used to  
18 track the movement of the actuator. A one-dimensional accelerometer mounted on the fast  
19 jaw was used to monitor the acceleration. A piezo load cell fixed below the bottom grip was  
20 utilized to measure the force transmitted. The signals of these transducers were connected  
21 to a data acquisition system with a sampling frequency of 65kHz. The deformation process  
22 of the PVB specimen was monitored by a high-speed camera (Phontron<sup>®</sup> Fastcam SA 1.1).  
23 The aperture of the lens was set to its widest opening, which is balanced with the exposure  
24 time. A 2000w halogen light M-300G by Leiyang<sup>®</sup> was used to provide lighting (Figure 6a).  
25 The frame rate was set to 1000~8000fps restricted by the testing speed and camera cache.  
26 The camera was synchronized with a TTL pulse from the Instron testing system. High-speed  
27 camera images were post-processed with an image tracking algorithm. The relative  
28 displacement time histories at the two black marking lines were used to determine the  
29 elongation of the specimen at its central testing region. The engineering strain was then  
30 calculated using the elongation divided by the original gauge length. The strain rate that  
31 each specimen experienced was derived through differentiating the strain history.

## 32 4.2 Results

33 High-speed tensile testing results on PVB material are presented in this section. An example  
34 of the test on PVB specimen (F07) with an actuator speed of 1m/s is shown to demonstrate



1 the specimen's deformation-to-failure process, and the strain rate history derived from high-  
2 speed camera images. The load time history and the way how inertia force is deducted is  
3 demonstrated. Validation of dynamic equilibrium for high-speed tensile test is carried out.  
4 Then, the testing results of all the PVB specimens are presented.

5

#### 6 4.2.1 Failure process

7 The deformation-to-failure process of specimen F07 is shown in Figure 8. All the images  
8 have been flipped from vertical to horizontal direction and stacked for demonstration  
9 convenience. At t=0ms the actuator was accelerating towards the designed testing velocity.  
10 The specimen was at rest as the fast jaw was not in contact yet. At t=11ms, the PVB  
11 specimen began to be stretched. The specimen deformed quickly under the tensile force. As  
12 can be observed, due to the substantial deformation of the specimen, even the two thin  
13 black reference markers were stretched. At t=111ms, the specimen experienced great  
14 elongation. Fracture initiated from its centre which splitted the specimen into halves. The  
15 machine came to a rest after the specimen broke.

16 The high-speed camera images were post-processed. The displacement trajectories at  
17 the two black markers were traced and used to form the specimen elongation history at its  
18 central testing gauge. The strain was derived by using the elongation divided by its original  
19 length between the two markers, and the strain rate history is calculated by differentiating  
20 the strain time history. As shown in Figure 9, the strain rate rises quickly to about  $60\text{s}^{-1}$  after  
21 the fast jaw gripped the clamping bar. A plateau is formed as the specimen was pulled at a  
22 constant 1m/s velocity. The specimen elongates at a relatively constant strain rate of  $60\text{s}^{-1}$   
23 until fracture occurs which is indicated on the strain rate history when it suddenly ascends  
24 due to the rebound of deformed specimen. The measured strain rate is a lot lower than the  
25 nominal strain rate ( $\dot{\epsilon}_{nom} \approx 100\text{s}^{-1}$ , estimated with the actuator velocity 1m/s dividing the  
26 testing gauge length of 10mm). This is because of deformation of PVB material at the  
27 shoulders of the tested specimen.

28

#### 29 4.2.2 Load time history

30 The load time history recorded by the load cell for specimen F07 is shown in Figure 10.  
31 The inertia force ( $F_{inertia}$ ) from the clamping devices is calculated by using the mass of clamps  
32 ( $m_{clamp}$ ) including both the alloy bars and the bolts times the recorded acceleration from the  
33 accelerometer ( $a$ ). The calculated inertia force is deducted from the total force ( $F_{total}$ ) to  
34 derive the net force ( $F_{net}$ ) experienced by the PVB specimen.

$$F_{inertia} = m_{clamp} \times a \quad (3)$$

$$F_{net} = F_{total} - F_{inertia}$$

1 As shown in Figure 10, the contribution of inertia force is negligible because of the light  
2 weight of the specially designed clamping device. In this way, the influence of inertia from  
3 the clamping devices is deducted, and the pure PVB material response is obtained for the  
4 high-speed test.

#### 5 4.2.3 Validation of high-speed test

6 In high-rate test the condition of dynamic stress equilibrium should be properly checked  
7 to ensure the validity of testing data. For high-speed test a sudden applied impulse can  
8 excite “system ringing”, which causes high amplitude stress oscillation and non-  
9 homogeneous deformation in the specimen [15]. It is therefore important to ensure stress  
10 wave travel in round trips for a sufficient number of times in the specimen to achieve stress  
11 uniformity in the specimen. The wave speed in the PVB specimen can be estimated using Eq.  
12 (2). For the PVB material with Young’s modulus 190MPa and density 1.07g/cm<sup>3</sup>, the wave  
13 speed in the specimen is about 421m/s. For a 20mm testing gauge length (between clamps)  
14 it takes about 47μs for the stress wave to propagate through the specimen. For the above  
15 specimen F07, the stress wave can propagate through the specimen for 78 times in round  
16 trips before it reaches the yielding point (according to load time history it takes about  
17 7.32ms), and about 1290 times before the specimen fractures (it takes about 121.29ms),  
18 which is more than sufficient to achieve stress equilibrium. Even at the maximum actuator  
19 pulling velocity of 20m/s performed in the present tests, it still takes about 0.21ms before it  
20 reached the yielding point, and about 4.11ms before the specimen fractures. The stress  
21 wave could travel within the specimen for more than twice before PVB yields, and about 44  
22 times round trips before the specimen fractures. It is therefore confident that the condition  
23 of stress equilibrium is satisfied in the high-speed tensile tests for the current study, and the  
24 testing results measured are valid.

25 To ensure valid testing results are obtained from the dynamic test, the response of the  
26 testing system should also be carefully checked. If the nature period of the system is not  
27 shorter than the rising time of the applied force onto the specimen, the force measured by  
28 the load cell will not properly track the real response of the specimen because of  
29 interactions. A load time history measured from the system after a specimen suddenly  
30 breaks is shown in Figure 11. It can be estimated that the nature oscillation period of the  
31 testing system is about 250μs. When the actuator was pulling at a velocity of 1m/s as shown  
32 above for specimen F07, the rising time of the tensile force to the point where the specimen  
33 initial yielded was approximately 6440μs, which was a lot longer than the nature period of

1 the system. When the actuator pulling velocity increases to 8m/s the rising time is about 870  
2  $\mu$ s. As the actuator velocity approaches the maximum velocity of 20m/s in the present tests,  
3 the rising time for the applied force to reach the yield stress is about twice the nature period  
4 of the system, which is the practical limit for the load cell being able to track the material  
5 response [9].

#### 6 4.2.4 Engineering stress versus engineering strain curves

7 Figure 12 shows the engineering stress vs. strain curves for the PVB specimens in the  
8 high-speed tests at actuator speeds varying from 0.1m/s to 20m/s. As can be observed, PVB  
9 material behaves very differently from that at quasi-static state. The stress shows a steep  
10 initial increase until a turning point from where the rise in stress slows down. The stress-  
11 strain curve depicts typical elasto-plastic like material property. However, the drop in  
12 modulus is not an actual sign that the material has yielded. Almost all the elongation of  
13 specimen was recovered after it fractured. Similar observations were also reported by  
14 previous researchers [9, 12]. It indicates that despite approximately an elasto-plastic model  
15 or a bilinear relationship with strain hardening can be used to describe the behavior of PVB  
16 under tension without unloading, the extension in PVB material is viscoelastic rather than  
17 plastic. If unloading behavior of PVB is to be considered, a bilinear viscoelastic model is  
18 preferable rather than an elasto-plastic model with hardening. It should be noted that due  
19 to testing difficulty there has not been any testing data reported in the literature yet on the  
20 unloading behavior of PVB at high strain rates. Therefore, the unloading path of PVB after  
21 dynamic tensile loading is still not properly understood. In this study, for easy demonstration  
22 of PVB mechanical behavior at high strain rate, a pseudo yield stress ( $\sigma_{ps,y}$ ) where material  
23 modulus change abruptly, and the corresponding strain - pseudo yield strain ( $\epsilon_{ps,y}$ ) are  
24 defined. The stress at failure  $\sigma_f$ , and the strain at failure  $\epsilon_f$  are calculated at the time when  
25 the specimen fractures. Two modulus are considered, the initial modulus  $E_{ini}$  which is  
26 defined as the gradient of a secant line through the pseudo yielding point and the origin on  
27 the engineering stress-strain curve, and the secondary modulus  $E_{sec}$  corresponding to the  
28 gradient between the pseudo yielding point and the ultimate failure point on the stress-  
29 strain curve. Table 2 summaries these testing results for the high-speed tensile test.

30 The engineering stress-strain curves for PVB in Figure 12 show that the response of PVB  
31 is very strain-rate dependent. When the actuator speed is 0.1m/s, which corresponds to a  
32 strain rate of about  $8s^{-1}$ , the behavior of the PVB is similar to viscoelastic material with large  
33 nonlinear deformation till the point of failure. As strain rate increases, the initial modulus  
34 increases. The pseudo yield stress also increases with strain rate. When the strain rate

1 increases from about  $8s^{-1}$  to over  $1300s^{-1}$ , the initial modulus increases from about 70MPa to  
2 120MPa, and the yield stress rises from about 3MPa to over 16MPa. It can also be observed  
3 that PVB material becomes less ductile at increased strain rates. The failure strain reduces  
4 from over 200% to 140% when the strain rate increases from  $8s^{-1}$  to  $1300s^{-1}$ . Oscillation was  
5 observed from the stress-strain curves as actuator speed increases above 6m/s, and  
6 becomes more apparent with the increase of the actuator speed. This is because of the  
7 relatively low strength of PVB material and the vibration of the testing system. The period of  
8 oscillation matches with the natural period of the load cell and the clamping device.

9

## 10 **5 Analysis and Discussion**

11 The testing results from both the low-speed and high-speed tensile tests are analyzed in the  
12 following section. Available testing data reported in the literature [9-12] are also included  
13 for the analysis. Discussions are made on the strain rate effect. Empirical formulae are  
14 derived from best fitting the testing results. It is worth noting that to be consistent with  
15 previous studies, in this section engineering stress and strain are utilized when analyzing the  
16 results.

### 17 **5.1 Strain rate effect**

18 Figure 13 illustrates selected engineering stress-strain curves of PVB at various strain  
19 rates. As can be seen, loading speed has very significant influence on the behaviors of PVB  
20 material. At a strain rate of  $0.019s^{-1}$ , PVB behaves essentially viscoelastic. As strain rate  
21 increases to  $0.198s^{-1}$ , PVB shows similar viscoelastic property but the initial stress rises  
22 quickly until a turning point. This phenomenon becomes more apparent when the strain rate  
23 increases to  $0.317s^{-1}$ . Under the tensile loading, the initial stress quickly jumps to about  
24 1.5MPa, and the fast increase in stress slows down and then increases in an exponential  
25 form with strain. As strain rate further increases, the pseudo yielding point becomes more  
26 and more apparent. The corresponding yield stress also increases with the strain rate. As  
27 shown after the pseudo yielding point the nonlinear behavior becomes less noticeable. PVB  
28 displays a bilinear viscoelastic property. The transition from nonlinear viscoelastic at low  
29 strain rate to bilinear viscoelastic is gradual. As strain rate increases, the pseudo yielding  
30 point becomes more and more apparent with higher pseudo yield stress at higher strain rate.  
31 After the pseudo yielding point the behavior of PVB gradually transforms from exponential  
32 viscoelastic to almost linear viscoelastic. As can be seen, the response of PVB specimen at  
33 strain rate  $7.7s^{-1}$  is still quite similar to those tested at low strain rates.

1 5.2 Pseudo yield stress and yield strain versus strain rate

2 The pseudo yielding point on the stress-strain curve is important to model the bilinear  
3 behavior of PVB material. The pseudo yield stress and strain from the current tests  
4 ( $\dot{\epsilon} \geq 0.198s^{-1}$ ) together with previous testing data reported in literature are summarized  
5 and plotted in Figure 14 and Figure 15 as a function of strain rate. The testing data from the  
6 current study show consistency with previous studies. As can be seen, the pseudo yield  
7 stress shows a clear trend of increase with strain rate. When the strain rate is about  $0.198s^{-1}$ ,  
8 the yield stress is about 0.5MPa. As strain rate increases to about  $8.6s^{-1}$ , the yield stress is  
9 about 4MPa. As strain rate becomes higher, the increase in the yield stress becomes faster.  
10 When the strain rate reaches to  $135s^{-1}$ , the yield stress is about 10MPa. The yield stress rises  
11 to about 20MPa at strain rate  $686s^{-1}$ . The increasing yield stress can therefore be  
12 approximated by a bilinear trend line as

$$\begin{aligned} \sigma_{yield} &= 1.689 + 1.573 \log_{10} \left( \frac{\dot{\epsilon}}{\dot{\epsilon}_0} \right) & \dot{\epsilon} \leq 10s^{-1} \\ \sigma_{yield} &= -4.533 + 8.351 \log_{10} \left( \frac{\dot{\epsilon}}{\dot{\epsilon}_0} \right) & \dot{\epsilon} > 10s^{-1} \end{aligned} \tag{4}$$

13 where  $\sigma_{yield}$  is the pseudo yields stress and  $\dot{\epsilon}$  is the strain rate.  $\dot{\epsilon}_0$  is a reference strain rate  
14 of  $1s^{-1}$ . The constants can be determined through nonlinear regression as presented in Eq.  
15 (4).

16 The pseudo yield strains of the current test fall in the range between 0.04 and 0.10. The  
17 yield strain appears to be steady in the tested strain rate range, which is also consistent with  
18 Bennison et al.'s testing data [11]. The measured yield strain values from Morison [12] and  
19 Hooper et al. [9] vary significantly. This can be attributed to the difficulties when measuring  
20 the very soft material PVB at high strain rate, and also the difficulty in properly defining the  
21 pseudo yielding point and therefore the yield strain.

22 5.2 Initial modulus versus strain rate

23 Figure 16 shows the tested initial modulus,  $E_{ini}$  of PVB material with respected to the  
24 strain rate. As can be observed, the initial modulus determined from the current test varies  
25 between 7MPa and 320MPa, which follows an increasing trend with strain rate. Under  
26 tensile loading, the initial modulus is only about 7MPa at a strain rate of about  $0.198s^{-1}$ . The  
27 initial modulus increases quickly as strain rate increases. At strain rate  $8s^{-1}$ , the modulus is  
28 about 30MPa, which rises to around 110MPa when strain rate is over  $70s^{-1}$ . As strain rate  
29 approaches  $1000s^{-1}$ , the initial modulus increases to about 300MPa. As pointed out by

1 Bennisson et al. [11] that by increasing the strain rate PVB shifts from a rubbery material,  
 2 essentially above its glass transition temperature, to a glassy elasto-plastic like material,  
 3 essentially below glass transition temperature. Except a couple of points provided by  
 4 Morison [12], the derived initial modulus in the current work agrees with the other previous  
 5 testing data. Significant variation can be noted between Morison's testing results  
 6 themselves around a strain rate about  $35s^{-1}$ . This is very likely to be resulted from the  
 7 difficulty involved in conducting high-speed tensile test on very soft material like PVB. These  
 8 contradictory points are excluded. Through best fitting the testing results, a bilinear  
 9 expression similar to that for the yield stress can be used to express the initial modulus

$$\begin{aligned}
 E_{ini} &= 25.648 + 11.608 \log_{10} \left( \frac{\dot{\epsilon}}{\dot{\epsilon}_0} \right) & \dot{\epsilon} \leq 10s^{-1} \\
 E_{ini} &= -92.275 + 129.490 \log_{10} \left( \frac{\dot{\epsilon}}{\dot{\epsilon}_0} \right) & \dot{\epsilon} > 10s^{-1}
 \end{aligned}
 \tag{5}$$

10 where  $E_{ini}$  is the initial modulus and  $\dot{\epsilon}$  is the strain rate.  $\dot{\epsilon}_0$  is a reference strain rate of  $1s^{-1}$ .  
 11 The constants in Eq. (5) are determined by nonlinear regression.

### 12 5.3 Failure stress and strain versus strain rate

13 The engineering failure stress and strain include both the low-speed and the high-speed  
 14 testing data are summarized and plotted in Figure 16 and Figure 17. Quasi-static tensile  
 15 testing results recently reported by Liu et al. [6] are also included in the analysis for  
 16 completeness. As shown in Figure 17, the failure stress of the current test shows obvious  
 17 strain-rate dependency. The failure stress increases from about 24MPa at a strain rate of  
 18  $0.008s^{-1}$  to about 30MPa at a strain rate of  $8s^{-1}$ . The dynamic increment effect becomes  
 19 more apparent as strain rate increases beyond  $10s^{-1}$ . When PVB material deforms at a strain  
 20 rate of  $1360s^{-1}$ , the failure stress increases to about 40MPa. The high-speed tensile testing  
 21 results show good consistency with Iwasaki et al.'s [10], Hooper et al.'s [9] and Bennisson et  
 22 al.'s [11] testing data. Variation in failure stress can be found on Morison's drop weight tests  
 23 [12], which vary from about 20MPa to 30MPa at a strain rate of  $30s^{-1}$ . The reason leading to  
 24 this variation is the interaction between the testing system and the specimen, as a result of  
 25 which the strain rate that material actually experienced is not as what was estimated. Large  
 26 variation can also be observed on the low-speed testing results in the current study. The  
 27 failure stresses of the low-speed tests fall in the range between 20MPa and 35MPa. Despite  
 28 the variation, an increasing trend can be observed with strain rate. A lot lower failure  
 29 stresses can be found on Liu et al.'s quasi-static testing results [6]. This is probably because  
 30 of premature failure of PVB specimens. Considering the above variations, Morison and Liu et

1 al.'s testing data are not included when data fitting the following empirical formula for  
 2 failure stress. A two-stage data-fit equation for the failure stress can be expressed as

$$\begin{aligned}\sigma_f &= 27.961 + 1.7753 \log_{10} \left( \frac{\dot{\varepsilon}}{\dot{\varepsilon}_0} \right) & \dot{\varepsilon} \leq 1s^{-1} \\ \sigma_f &= 30.698 + 2.3415 \log_{10} \left( \frac{\dot{\varepsilon}}{\dot{\varepsilon}_0} \right) & \dot{\varepsilon} > 1s^{-1}\end{aligned}\quad (6)$$

3 where  $\dot{\varepsilon}_0$  is a reference strain rate  $\dot{\varepsilon}_0$  of  $1s^{-1}$ .

4 The failure strains measured in the current test are consistent with most of previous  
 5 testing results [6, 9-11] at both the quasi-static and dynamic regions. The results provided by  
 6 Morison [12] are however lower than the current testing data. This is likely due to the  
 7 different testing technique utilized to measure the specimen displacement. In his dynamic  
 8 tensile test, Morison adopts the machine actuator displacement to evaluate the specimen  
 9 strain. Because of the deformation of specimen at shoulder, the strain at the central testing  
 10 gauge is greatly underestimated. In contrast, in this study the specimen extension and strain  
 11 are traced by optical device targeting at the central region of the specimen only. More  
 12 accurate testing results are believed to be obtained in the current test. As shown in Figure  
 13 18, the failure strain decreases with the increased strain rate, indicating PVB material  
 14 becomes less ductile as pulling speed increases. At a strain rate of about  $0.01s^{-1}$ , failure  
 15 occurs when strain is nearly 300%. The failure strain reduces to about 220% at a strain rate  
 16 of  $0.2s^{-1}$ . When the strain rate is above  $100s^{-1}$ , the failure strain reduces to below 200%. At a  
 17 strain rate of  $700s^{-1}$ , the failure strain plummets to only 150%. An expression of Eq. (7) can  
 18 be used to approximate the failure strain

$$\varepsilon_f = \varepsilon_{f0} - m_f \log_{10} \left( \frac{\dot{\varepsilon}}{\dot{\varepsilon}_0} \right) \quad (7)$$

19 where  $\varepsilon_f$  and  $\dot{\varepsilon}$  represent the engineering failure strain and strain rate,  $m_f$  is a constant, and  
 20  $\varepsilon_{f0}$  is the failure strain at the reference strain rate  $\dot{\varepsilon}_0$  of  $1s^{-1}$ . Nonlinear regression finds  $\varepsilon_{f0}$   
 21 to be  $2.198 \pm 0.024$ , and  $m_f = -0.1176 \pm 0.013$ .

22 Figure 19 shows the derived secondary modulus at various strain rates. As shown the  
 23 values of the secondary modulus vary in the range of 9MPa to 16MPa, and appear to be  
 24 steady with respect to the strain rate. A slight decrease in secondary modulus with respect  
 25 to the rise of strain rate can be found after data fitting. The derived secondary modulus is  
 26 consistent with the scatters from the other researchers [9-12]. It is worth noting that  
 27 different from the secant secondary modulus we use herein, considering the hyperelastic  
 28 nonlinear deformation of PVB right from its pseudo yielding point, Hooper et al. [9]

1 introduce the modulus  $E_{20}$  which corresponds to the gradient of the stress-strain curve at 20%  
2 strain. As shown in Figure 19, the data of  $E_{20}$  from Hooper et al. is lower than the plastic  
3 modulus we defined above. Excluding the data of  $E_{20}$ , the testing data are fitted to form the  
4 empirical formula of the plastic modulus of PVB as

$$E_{sec} = E_0 + m_e \log_{10} \left( \frac{\dot{\epsilon}}{\dot{\epsilon}_0} \right) \quad (8)$$

5 where  $E_{sec}$  and  $\dot{\epsilon}$  stand for the secondary modulus and strain rate;  $m_e$  is a constant and  $E_0$  is  
6 the secondary modulus at the reference strain rate  $\dot{\epsilon}_0$  of  $1s^{-1}$ . The constants were  
7 determined using nonlinear regression and were found to be  $E_0=13.971MPa \pm 0.399MPa$ ,  
8 and  $m_e=-0.432MPa \pm 0.223MPa$ .

## 9 **6 Conclusion**

10 In this paper we present laboratory tests to study the dynamic material properties of  
11 polymer material PVB. Low-speed and high-speed uniaxial tensile tests were carried out on  
12 PVB specimens covering a wide strain rate range from  $0.008s^{-1}$  to  $1360s^{-1}$ . The engineering  
13 stress-strain curves obtained show that PVB exhibits viscoelastic material property under  
14 quasi-static loading. As strain rate increases, it transfers into a bilinear viscoelastic material  
15 which appears to be similar to elasto-plastic material. The pseudo yield stress increases with  
16 strain rate from about 3MPa at a strain rate of  $8s^{-1}$  to nearly 20MPa at a strain rate of  $1360s^{-1}$ .  
17 As strain rate increases no significant increment was found on the corresponding yield  
18 strain. The increase in yield stress was mainly attributed to increment in initial modulus. It  
19 was also found that the engineering stress to failure varied from 24MPa at a strain rate of  
20  $0.008s^{-1}$  to about 40MPa at  $1360s^{-1}$ . The failure strain was found to vary between 280% at  
21  $0.008s^{-1}$  to about 140% at a strain rate of  $1360s^{-1}$  showing a decreasing trend over the tested  
22 strain rate range. The secondary modulus of PVB material for the dynamic test was found  
23 insensitive to strain rate, which vary in the range of 9MPa and 16MPa. The current testing  
24 results were analysed together with previous testing data on PVB. Empirical formulae are  
25 derived through best fitting the testing data.

## 26 **Acknowledgement**

27 The authors would like to thank Australian Research Council for financial support. The  
28 contributions of final year student Mr. Todd Learmonth from the University of Western  
29 Australia and Mr. Xuejie Zhang from Tianjin University in conducting laboratory tests are  
30 acknowledged. We also acknowledge the supports from Cooling Brothers® Glass Company



1 for providing testing materials. The first author would like to acknowledge the Ad Hoc  
2 scholarship from the University of Western Australia.

### 3 **Reference**

- 4 [1] X. Zhang, H. Hao, G. Ma, Parametric study of laminated glass window response to blast  
5 loads, *Engineering Structures*, 56 (2013) 1707-1717.
- 6 [2] X. Zhang, H. Hao, G. Ma, Laboratory test and numerical simulation of laminated glass  
7 window vulnerability to debris impact, *International Journal of Impact Engineering*, 55 (2013)  
8 49-62.
- 9 [3] M. Larcher, G. Solomos, F. Casadei, N. Gebbeken, Experimental and numerical  
10 investigations of laminated glass subjected to blast loading, *International Journal of Impact*  
11 *Engineering*, 39 (2012) 42-50.
- 12 [4] X. Zhang, H. Hao, Experimental Study of Laminated Glass Window Responses under  
13 Impulsive and Blast Loading, in press with *International Journal of Impact Engineering*,  
14 (2014).
- 15 [5] J. Xu, Y. Li, D. Ge, B. Liu, M. Zhu, Experimental investigation on constitutive behavior of  
16 PVB under impact loading, *International Journal of Impact Engineering*, 38 (2011) 106-114.
- 17 [6] B. Liu, Y. Sun, Y. Li, Y. Wang, D. Ge, J. Xu, Systematic experimental study on mechanical  
18 behavior of PVB (polyvinyl butyral) material under various loading conditions, *Polymer*  
19 *Engineering & Science*, 52 (2012) 1137-1147.
- 20 [7] A.V. Duser, A. Jagota, S.J. Bennison, Analysis of glass/polyvinyl butyral laminates  
21 subjected to uniform pressure, *Journal of engineering mechanics*, 125 (1999) 435-442.
- 22 [8] S.J. Bennison, A. Jagota, C.A. Smith, Fracture of glass/poly (vinyl butyral)(Butacite®)  
23 laminates in biaxial flexure, *Journal of the American Ceramic Society*, 82 (1999) 1761-1770.
- 24 [9] P. Hooper, B. Blackman, J. Dear, The mechanical behaviour of poly (vinyl butyral) at  
25 different strain magnitudes and strain rates, *Journal of Materials Science*, 47 (2012) 3564-  
26 3576.
- 27 [10] R. Iwasaki, C. Sato, J. Latailladeand, P. Viot, Experimental study on the interface fracture  
28 toughness of PVB (polyvinyl butyral)/glass at high strain rates, *International Journal of*  
29 *Crashworthiness*, 12 (2007) 293-298.
- 30 [11] S. Bennison, J. Sloan, D. Kistunas, P. Buehler, T. Amos, C. Smith, Laminated glass for  
31 blast mitigation: Role of interlayer properties, in: *Proceedings of Glass Processing Days*,  
32 Tampere, Finland, 2005.
- 33 [12] C. Morison, The resistance of laminated glass to blast pressure loading and the  
34 coefficients for single degree of freedom analysis of laminated glass, PhD thesis, Cranfield  
35 University (2010).
- 36 [13] W.N. Sharpe Jr, W.N. Sharpe, Springer handbook of experimental solid mechanics,  
37 Springer, 2008.
- 38 [14] X. Zhang, Y. Zou, H. Hao, X. Li, G. Ma, K. Liu, Laboratory Test on Dynamic Material  
39 Properties of Annealed Float Glass, *International Journal of Protective Structures*, 3 (2012)  
40 407-430.
- 41 [15] X. Xiao, Dynamic tensile testing of plastic materials, *Polymer Testing*, 27 (2008) 164-178.

42  
43

- 1 Table 1 Summary of low-speed testing results
- 2 Table 2 Summary of high-speed tensile testing results
- 3
- 4

Specimen No.	Testing machine	Engineering strain rate (s <sup>-1</sup> )	Engineering failures strain	Engineering failure stress (MPa)
G04	Baldwin	0.008	2.805	24.022
G10	Baldwin	0.009	2.543	21.260
G05	Baldwin	0.016	2.637	32.849
G06	Baldwin	0.020	2.610	30.722
G15	Baldwin	0.038	2.500	31.596
G16	Baldwin	0.039	2.506	31.828
G12	Baldwin	0.040	2.420	28.140
G11	Baldwin	0.043	2.420	27.907
G20	INSTRON	0.020	2.805	24.022
G21	INSTRON	0.020	2.454	27.163
G35	INSTRON	0.099	2.512	33.408
G36	INSTRON	0.099	2.322	27.528
G37	INSTRON	0.099	1.974	20.341
G38	INSTRON	0.099	2.362	29.710
G25	INSTRON	0.198	2.223	34.311
G40	INSTRON	0.198	2.223	33.348
G26	INSTRON	0.198	2.282	33.138
G34	INSTRON	0.198	2.262	31.558
G27	INSTRON	0.317	1.747	25.308
G31	INSTRON	0.317	1.874	27.499
G32	INSTRON	0.317	1.747	23.348
G33	INSTRON	0.317	1.766	23.944
G28	INSTRON	0.317	2.004	31.787

Table 1 Summary of low-speed testing results

1

2

Specimen No.	Actuator speed m/s	Engineering Strain rate $s^{-1}$	Engineering $\sigma_{ps,y}$ MPa	Engineering $\epsilon_{ps,y}$	$E_{ini}$ MPa	Engineering $\sigma_f$ MPa	Engineering $\epsilon_f$	$E_{sec}$ MPa
F01	0.1	8.6	2.05	0.07	30.52	28.90	2.01	14.38
F02	0.1	7.7	3.40	0.05	73.51	29.02	2.08	13.94
F03	0.5	44.7	4.42	0.05	93.76	32.96	2.02	16.35
F04	1	116.7	6.49	0.07	91.08	34.47	2.01	17.16
F05	1	67.3	7.19	0.08	88.83	32.01	2.02	15.87
F06	1	62.3	6.78	0.05	127.43	33.80	1.95	17.33
F07	1	61.1	9.27	0.08	116.38	34.69	1.95	17.83
F08	2	134.5	10.79	0.08	130.61	37.81	1.93	19.62
F09	2	134.5	9.81	0.07	145.32	36.40	1.91	19.03
F10	3	154.8	12.05	0.07	162.57	35.43	1.79	19.84
F11	4	245.2	11.49	0.06	183.53	38.76	1.73	22.44
F12	5	269.8	11.24	0.05	224.06	38.93	1.81	21.55
F13	6	310.2	12.61	0.04	320.00	40.26	1.69	23.83
F14	7	329.9	16.22	0.05	307.28	40.56	1.72	23.55
F15	8	395.9	18.41	0.07	274.76	32.95	1.80	18.31
F16	10	460.7	20.63	0.09	218.96	37.51	1.71	10.47
F17	15	685.7	24.32	0.09	257.17	39.71	1.51	10.84
F18	20	1360.0	21.81	0.07	306.33	38.90	1.40	12.87

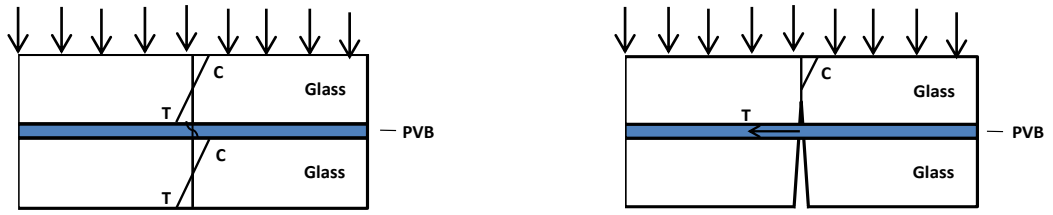
Table 2 Summary of high-speed tensile testing results

1

2

3

- 1 Figure 1 Load carrying diagram of laminated glass
- 2 Figure 2 Illustration of specimen geometry for low-speed test
- 3 Figure 3 Baldwin and Intron hydraulic machines for low-speed test
- 4 Figure 4 Sample strain-rate time history for low-speed test derived from crosshead
- 5 displacement
- 6 Figure 5 Stress-strain curves of low-speed tensile tests at different strain rates
- 7 Figure 6 High-speed testing system and clamping devices
- 8 Figure 7 Illustration of specimen geometry
- 9 Figure 8 High-speed camera images on specimen F07 deformation-to-failure process
- 10 Figure 9 Strain-rate time history of specimen F07 in high-speed tensile test
- 11 Figure 10 Load time histories of machine load, inertia force, and net force on material for
- 12 specimen F07
- 13 Figure 11 Free vibration of the testing system after a specimen fractures
- 14 Figure 12 Stress-strain curves of PVB in high-speed tensile tests at different pulling speeds
- 15 Figure 13 Illustration of strain rate effect on engineering stress-strain curves
- 16 Figure 14 Pseudo yield stress vs. strain rate
- 17 Figure 15 Pseudo yield strain vs. strain rate
- 18 Figure 16 Initial modulus vs strain rate
- 19 Figure 17 Engineering failure stress vs. strain rate
- 20 Figure 18 Engineering failure strain vs strain rate
- 21 Figure 19 Secondary modulus vs. strain rate
- 22



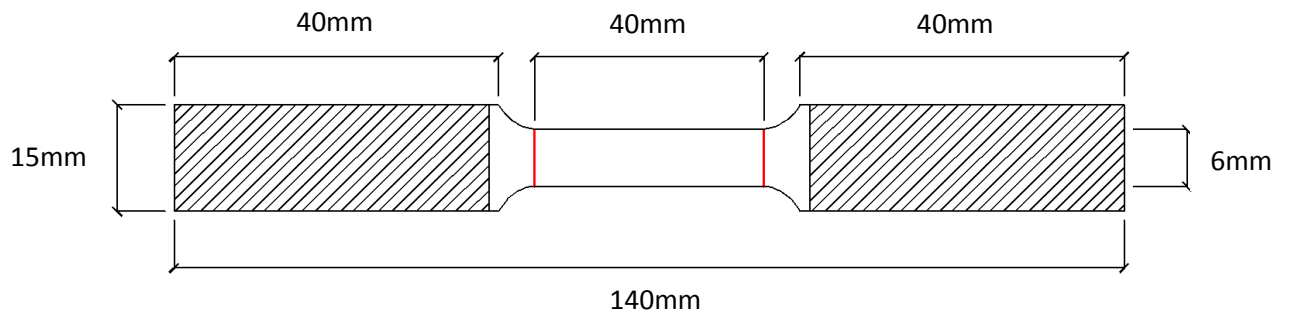
a) Pre-glass ply breakage

b) Post-glass ply breakage

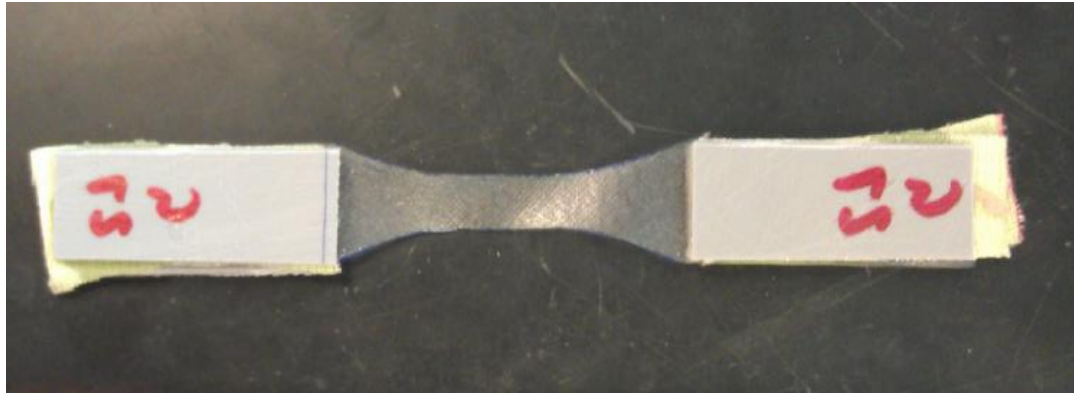
Figure 1 Load carrying diagram of laminated glass

1

2



1



2

3

Figure 2 Illustration of specimen geometry for low-speed test

4



a) Baldwin machine



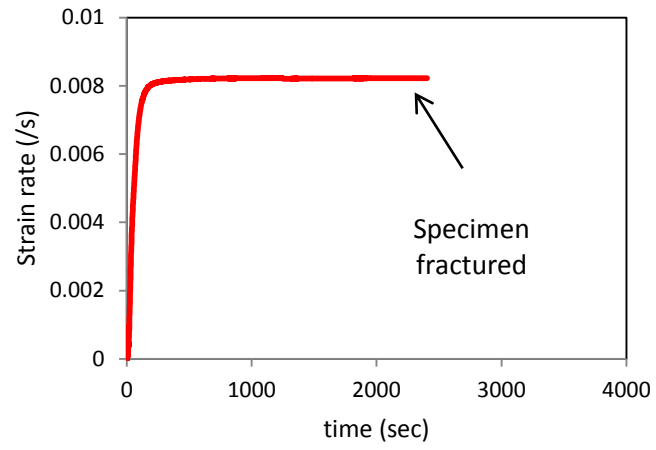
b) Instron machine

Figure 3 Baldwin and Intron hydraulic machines for low-speed test

1

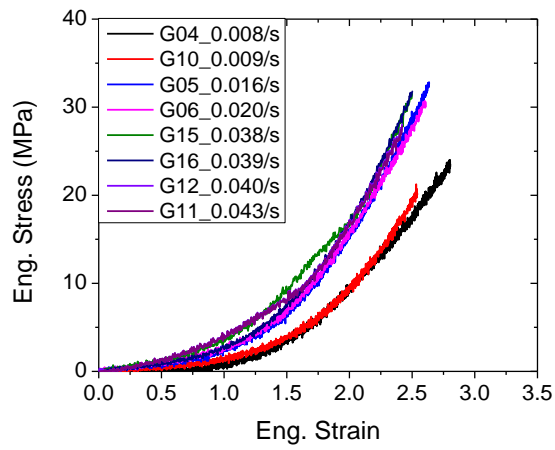
2



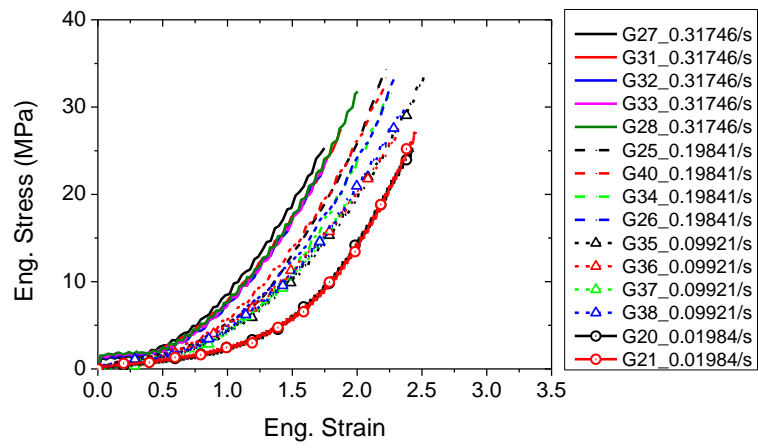


1  
2  
3

Figure 4 Sample strain-rate time history for low-speed test derived from crosshead displacement



a) Baldwin

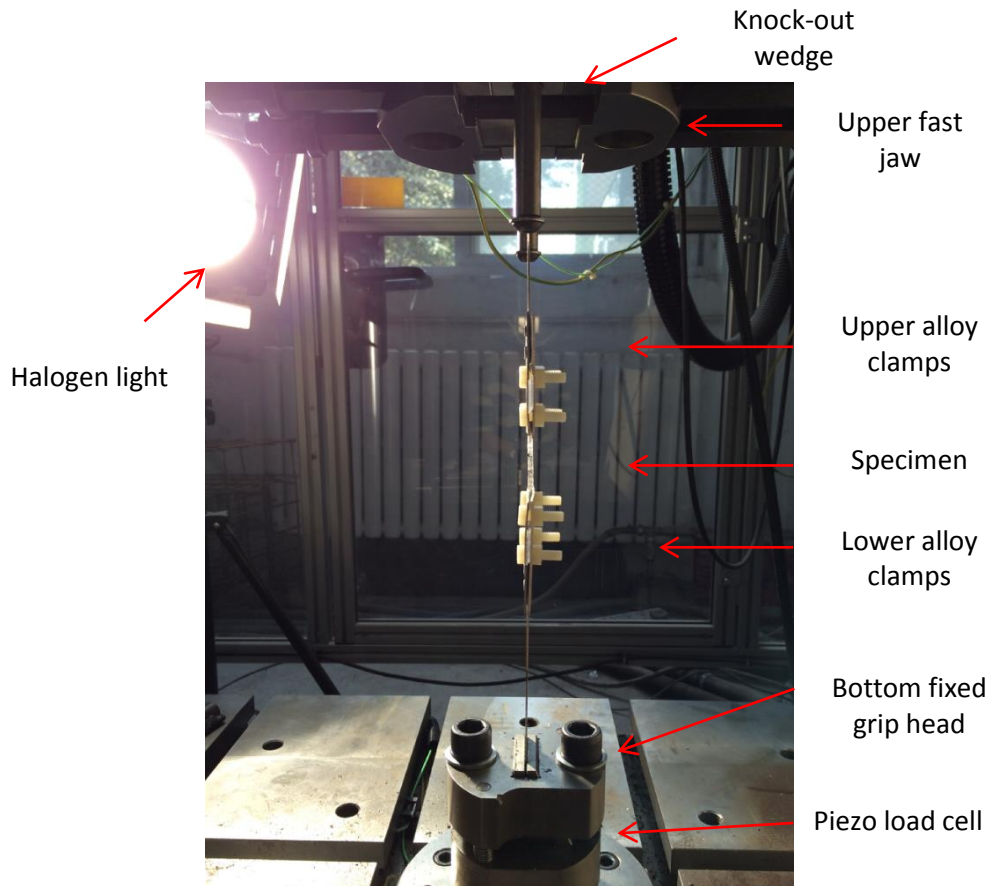


b) Instron

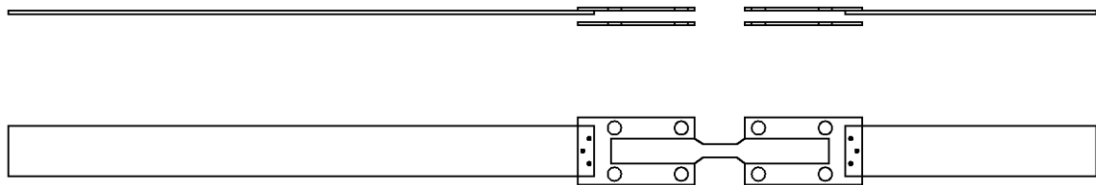
1

Figure 5 Stress-strain curves of low-speed tensile tests at different strain rates

2



a) Image of high-speed test setup



b) Illustration of clamps

Figure 6 High-speed testing system and clamping devices

1

2

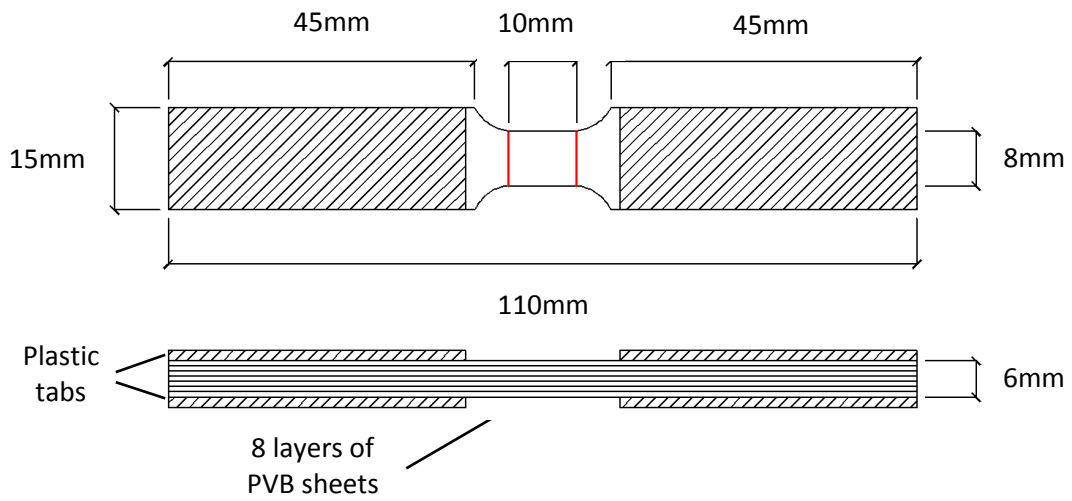

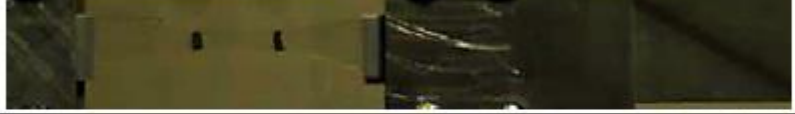
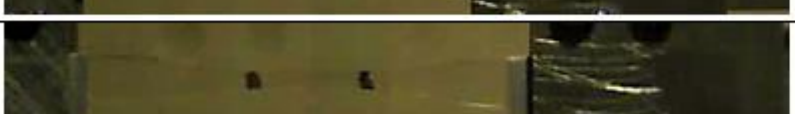


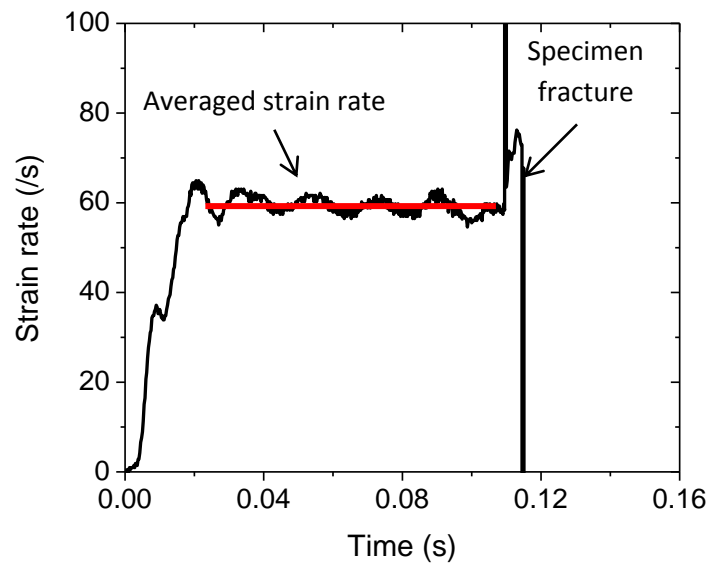
Figure 7 Illustration of specimen geometry

- 1
- 2
- 3

	t=0ms
	t=11ms
	t=41ms
	t=56ms
	t=71ms
	t=85ms
	t=111ms
	t=112ms

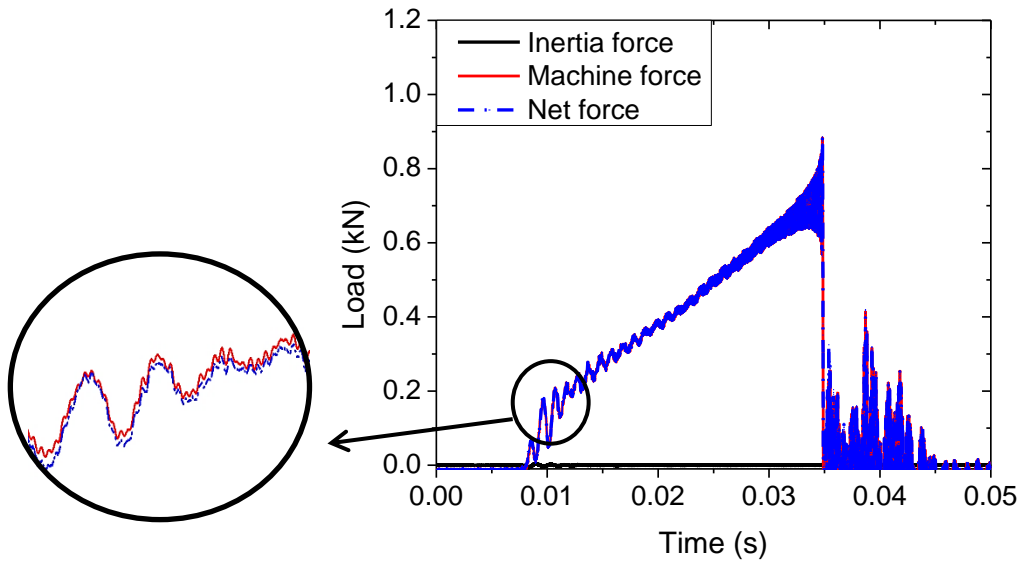
1  
2  
3

Figure 8 High-speed camera images on specimen F07 deformation-to-failure process



- 1
- 2
- 3

Figure 9 Strain-rate time history of specimen F07 in high-speed tensile test



- 1
- 2
- 3
- 4

Figure 10 Load time histories of machine load, inertia force, and net force on material for specimen F07

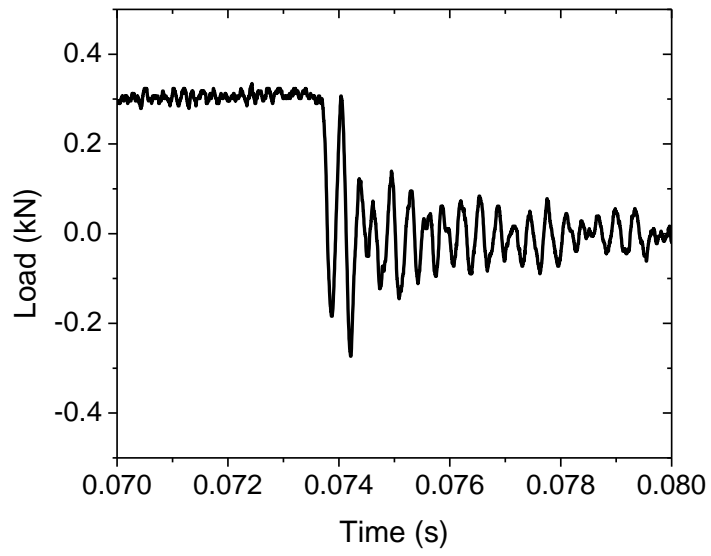
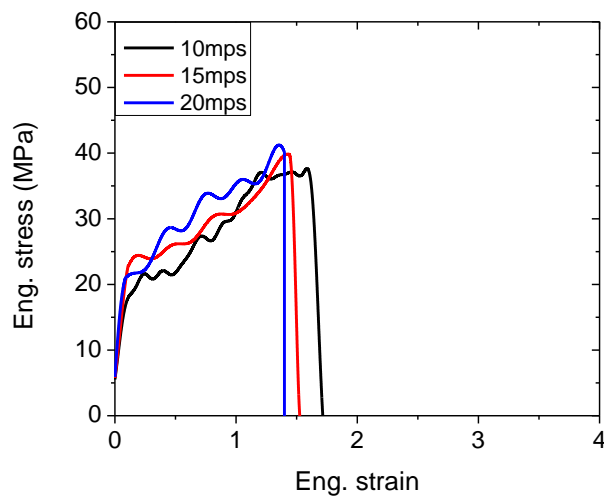
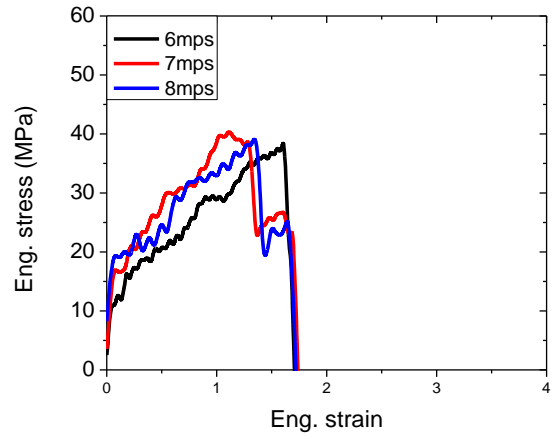
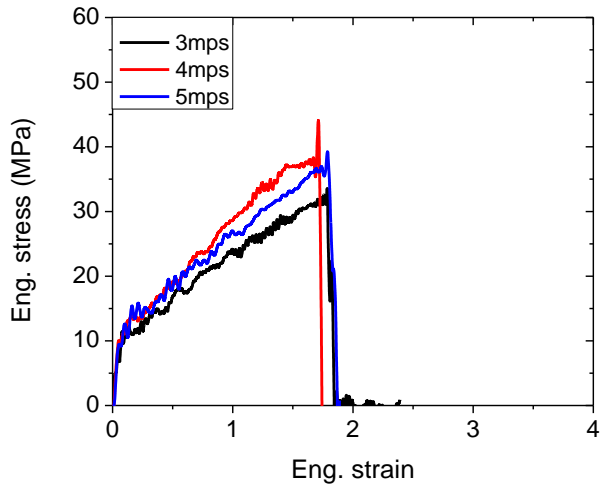
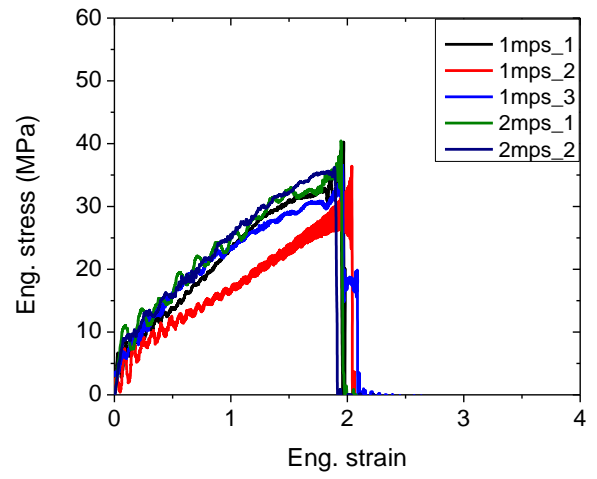
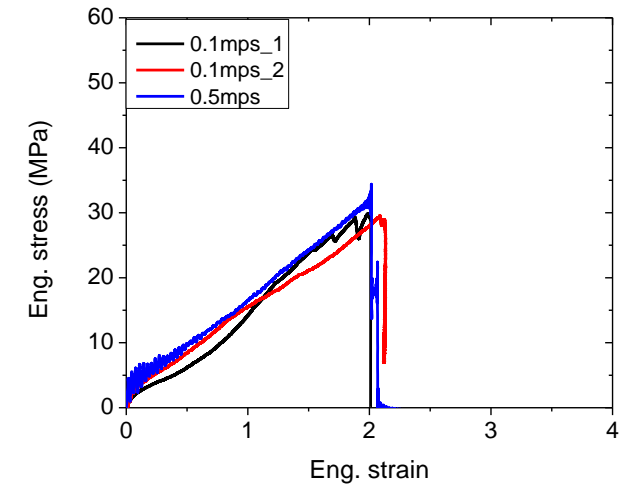


Figure 11 Free vibration of the testing system after a specimen fractures

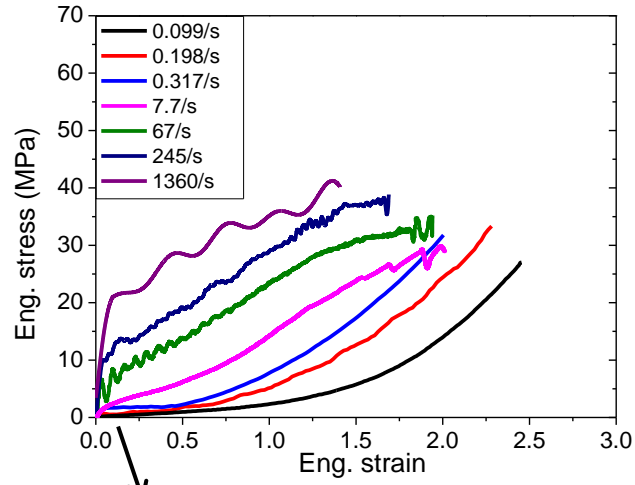
- 1
- 2
- 3



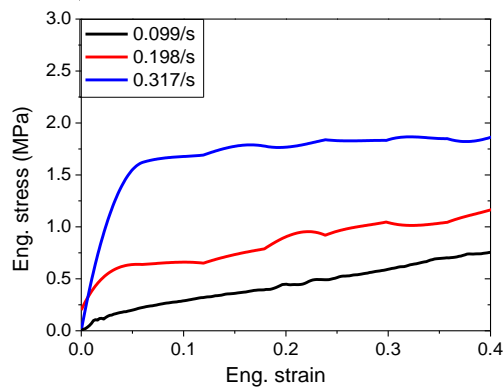


1 **Figure 12 Stress-strain curves of PVB in high-speed tensile tests at different pulling speeds**

2



1

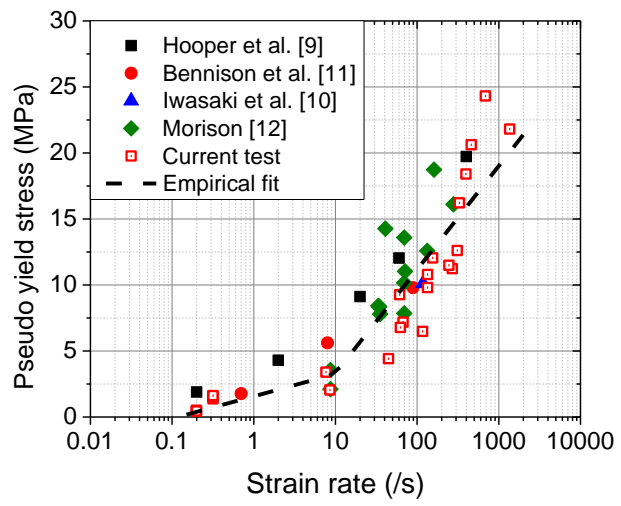


2

3

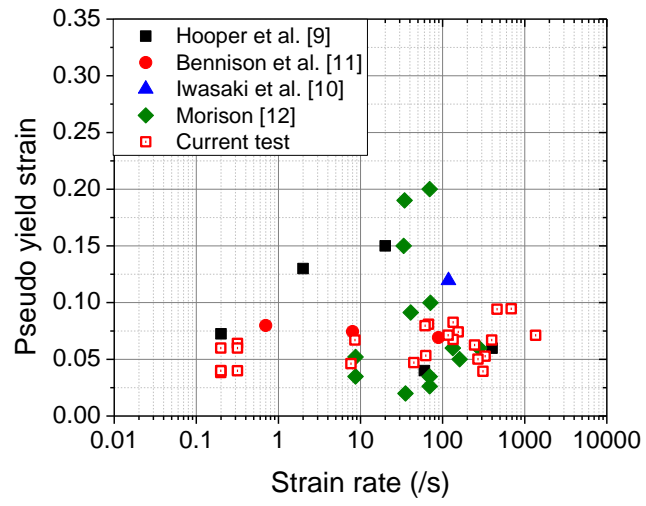
Figure 13 Illustration of strain rate effect on engineering stress-strain curves

4



- 1
- 2
- 3

Figure 14 Pseudo yield stress vs. strain rate

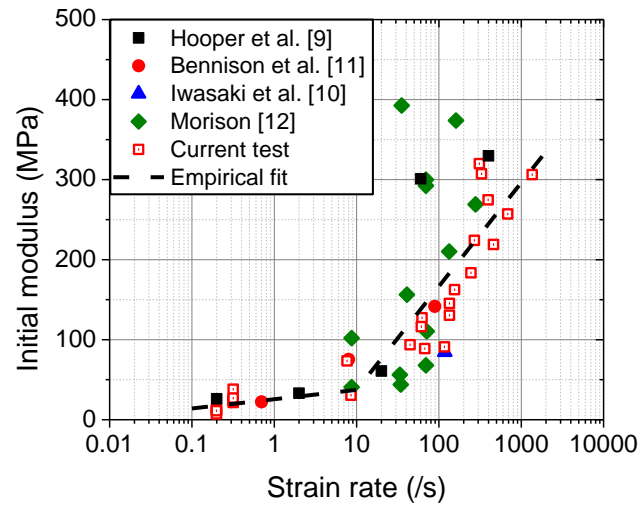


1

2

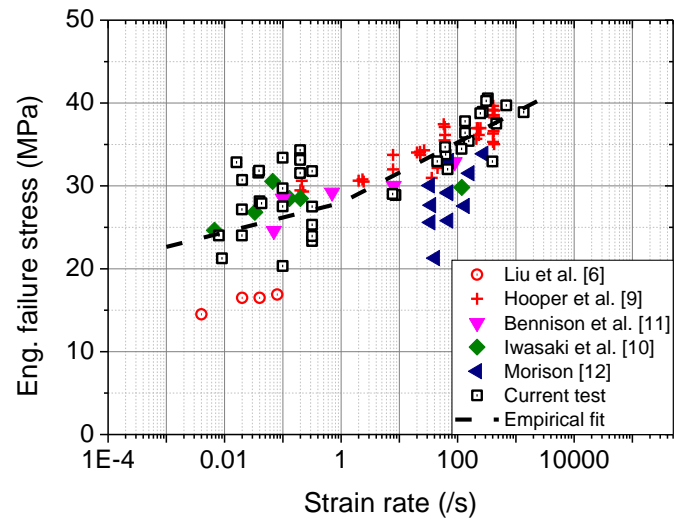
Figure 15 Pseudo yield strain vs. strain rate

3



1  
2  
3

Figure 16 Initial modulus vs strain rate

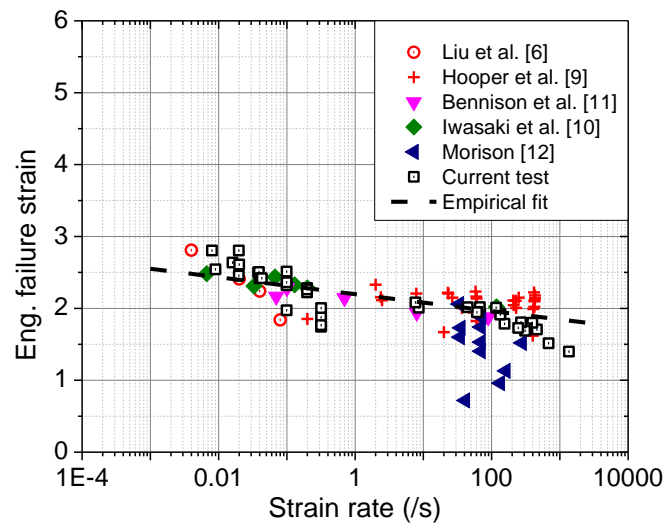


1

2

3

Figure 17 Engineering failure stress vs. strain rate

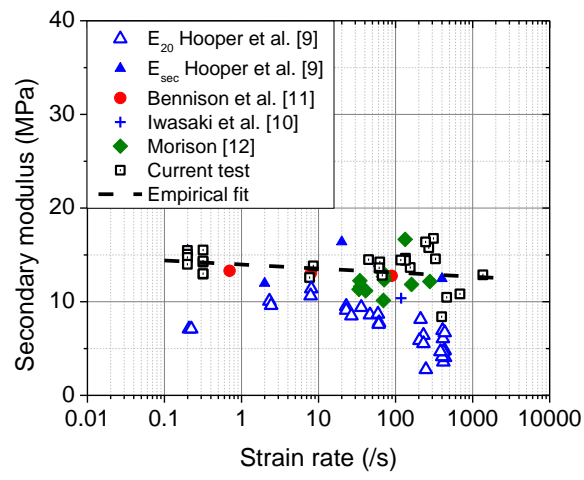


1

2

3

Figure 18 Engineering failure strain vs strain rate



1

2

3

4

Figure 19 Secondary modulus vs. strain rate